

DESY 96-216

ISSN 0418-9833

October 1996

Electroweak Phase Transition and Neutrino Masses*

W. Buchmüller

Deutsches Elektronen-Synchrotron DESY, 22603 Hamburg, Germany

Abstract

The presently observed cosmological baryon asymmetry has been finally determined at the time of the electroweak phase transition, when baryon and lepton number violating interactions fell out of thermal equilibrium. We discuss the thermodynamics of the phase transition based on the free energy of the SU(2) Higgs model at finite temperature, which has been studied in perturbation theory and lattice simulations. The results suggest that the baryon asymmetry has been generated by lepton number violating interactions in the symmetric phase of the standard model, i.e., at temperatures above the critical temperature of the electroweak transition. The observed value of the baryon asymmetry, $n_B/s \sim 10^{-10}$, is naturally obtained in an extension of the standard model with right-handed neutrinos where $B - L$ is broken at the unification scale $\Lambda_{\text{GUT}} \sim 10^{16}$ GeV. The corresponding pattern of masses and mixings of the light neutrinos ν_e , ν_μ and ν_τ is briefly described.

*To be published in *Quarks '96*, Proc. of the IXth International Seminar, Yaroslavl, Russia, 1996

1 Introduction

In the standard model of electroweak interactions all masses are generated by the Higgs mechanism. As a consequence, at high temperatures a transition occurs from a massive low-temperature phase to a ‘massless’ high-temperature phase, where the Higgs vacuum expectation value ‘evaporates’ and the electroweak symmetry is ‘restored’ [1].

Due to the chiral nature of the weak interactions baryon number (B) and lepton number (L) are not conserved in the standard model [2]. At zero temperature this has no observable effect due to the smallness of the weak coupling. However, as the temperature approaches the critical temperature T_c of the electroweak phase transition, B and L violating processes come into thermal equilibrium [3]. Their rate is determined by the free energy of sphaleron-type field configurations which carry topological charge. In the standard model they induce an effective interaction of all left-handed fermions (cf. Fig. 1) which violates baryon and lepton number by three units,

$$\Delta B = \Delta L = 3. \quad (1)$$

Since B and L violating processes fall out of thermal equilibrium below T_c , the

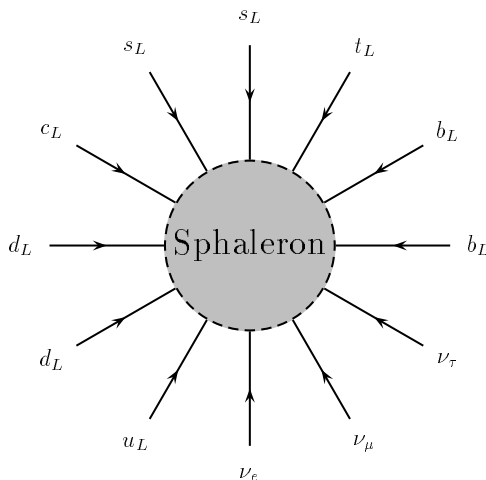


Figure 1: One of the 12-fermion processes which are in thermal equilibrium in the high-temperature phase of the standard model.

presently observed value of the baryon asymmetry of the universe has finally been determined at the electroweak transition. Hence, the study of the thermodynamics of this transition is of great cosmological significance.

Sphaleron processes conserve $B - L$. In the high-temperature, ‘symmetric’ phase, where B and L violating processes are expected to stay in thermal equilibrium over

a wide range of temperatures, the expectation values of B and L are related,

$$\langle B \rangle_T \simeq C \langle B - L \rangle_T \simeq \frac{C}{C-1} \langle L \rangle_T, \quad (2)$$

where $C = \frac{28}{79}$ in the standard model [4]. Hence, baryon and lepton number are correlated in the symmetric phase, and the generation of a baryon asymmetry requires lepton number violation.

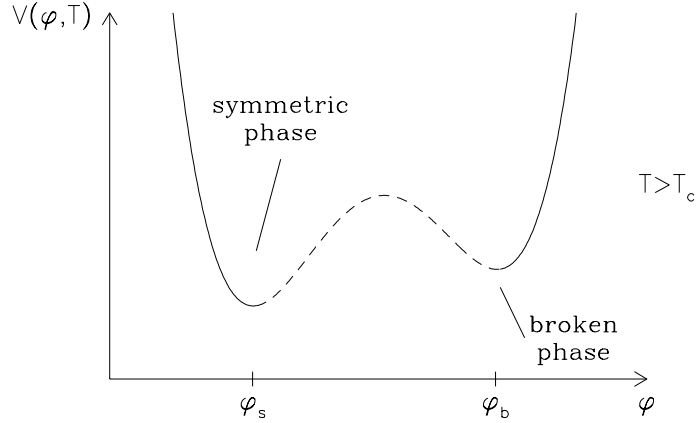


Figure 2: Free energy as function of the order parameter at a temperature slightly above the critical temperature of a first-order phase transition.

In the abelian Higgs model, i.e., scalar electrodynamics, the high-temperature phase transition is known to be of first order for sufficiently small Higgs masses [5, 6]. The expectation value of the Higgs field plays the role of an order parameter. At temperatures just above the critical temperature T_c the Higgs phase is metastable. It decays in a first-order transition to the symmetric phase, which is accompanied by a jump in the order parameter $\Delta v = v_b - v_s$ (cf. Fig. 2).

A similar behaviour is expected in the standard model, with a critical temperature given by the Fermi constant, $T_c \sim G_F^{-1/2}$. In a first-order phase transition a strong deviation from thermal equilibrium can occur. Since the standard model contains CP violating and, at high temperatures, also B violating interactions, all conditions for baryogenesis are fulfilled. It is therefore conceivable that the cosmological baryon asymmetry has indeed been generated at the electroweak phase transition [7]. Such a scenario requires that a produced baryon asymmetry is not erased by the sphaleron processes in the Higgs phase close to the critical temperature. From this condition a lower bound on the jump of order parameter at the phase transition can be derived (see [7]),

$$\frac{\Delta v(T_c)}{T_c} > 1.2. \quad (3)$$

This condition is necessary for electroweak baryogenesis although far from sufficient. A discussion of the complicated nonequilibrium processes in the electroweak plasma can be found in [7].

In order to examine whether condition (3) is satisfied, one has to study the thermodynamics of the electroweak transition near the critical temperature. Here the main obstacle are the well known infrared divergencies of non-abelian gauge theories at high temperature. As a first step towards a treatment of the full standard model the following simplifications are usually made: fermions are integrated out using high-temperature perturbation theory, and the electromagnetic interaction is neglected ($\sin \Theta_W = 0$). One is then left with the SU(2) Higgs model.

2 Thermodynamics of the SU(2) Higgs model

The observables which characterize a first-order phase transition are critical temperature, jump in the order parameter and latent heat. Also important are surface tension and correlation lengths which are more difficult to compute and which we shall not discuss in detail. Our analysis will be based on the gauge invariant ‘order parameter’ $\langle \Phi^\dagger \Phi \rangle$ and the corresponding free energy computed in lattice simulations and perturbation theory. In our discussion we shall closely follow [8].

It is well known that the electroweak phase transition is influenced by non-perturbative effects whose size is governed by the confinement scale of the effective three-dimensional theory which describes the high-temperature limit of the SU(2) Higgs model. These effects are particularly relevant in the symmetric phase, and one may worry to what extent a perturbative analysis of the phase transition can yield sensible results. As we shall see, perturbation theory is self-consistent at two-loop order. A comparison with results obtained by lattice simulations will then enable us to estimate the effect of non-perturbative corrections.

Generalities

The action of the SU(2) Higgs model at finite temperature T reads

$$S_\beta[\Phi, W] = \int_\beta dx \, \text{Tr} \left[\frac{1}{2} W_{\mu\nu} W_{\mu\nu} + (D_\mu \Phi)^\dagger D_\mu \Phi + \mu \Phi^\dagger \Phi + 2\lambda (\Phi^\dagger \Phi)^2 \right], \quad (4)$$

with

$$\Phi = \frac{1}{2}(\sigma + i\vec{\pi} \cdot \vec{\tau}), \quad D_\mu \Phi = (\partial_\mu - igW_\mu)\Phi, \quad W_\mu = \frac{1}{2}\vec{\tau} \cdot \vec{W}_\mu, \quad (5)$$

$$\int_\beta dx = \int_0^\beta d\tau \int_\Omega d^3x, \quad \beta = \frac{1}{T}. \quad (6)$$

Here \vec{W}_μ is the vector field, σ is the Higgs field, $\vec{\pi}$ is the Goldstone field, $\vec{\tau}$ is the triplet of Pauli matrices, and Ω is the spatial volume. For perturbative calculations gauge fixing and ghost terms have to be added to the action (4).

The free energy density of the system, $W(T, J)$, is given by the partition function, i.e., the trace of the density matrix,

$$\exp(-\beta\Omega W(T, J)) = \text{Tr} \exp \left[-\beta \left(\hat{H} + J \int_{\Omega} d^3x \hat{\Phi}^\dagger \hat{\Phi} \right) \right] , \quad (7)$$

where \hat{H} is the Hamilton operator of the theory, and $\hat{\Phi}$ is the operator describing the Higgs field. We have added a source J , with $\partial_\mu J = 0$, coupled to the spatial average of the gauge invariant composite operator $\hat{\Phi}^\dagger \hat{\Phi}$ (here and below the trace operator acting on $\hat{\Phi}^\dagger \hat{\Phi}$ is omitted for brevity). The partition function can be expressed as a euclidian functional integral (see [9]),

$$\exp(-\beta\Omega W(T, J)) = \int_{\beta} D\Phi D\Phi^\dagger DW_\mu \exp \left(- \int_{\beta} dx \left(L + J\Phi^\dagger \Phi \right) \right) , \quad (8)$$

where L is the euclidean lagrangian density, and the bosonic fields Φ and W_μ satisfy periodic boundary conditions at $\tau = 0$ and $\tau = \beta$. Eq. (8) is the starting point of perturbative as well as numerical evaluations of the free energy.

Note, that the source J in Eq. (8) couples to a gauge invariant composite field. Hence, the free energy $W(T, J)$ is gauge independent. The spatially constant source J simply redefines the mass term in the action (4). This is in contrast to the usually considered generating function of connected Green functions at zero momentum,

$$\exp(-\beta\Omega \tilde{W}(T, j; J)) = \int_{\beta} D\Phi D\Phi^\dagger DW_\mu \exp \left(- \int_{\beta} dx \left(L + J\Phi^\dagger \Phi + j\sigma \right) \right) . \quad (9)$$

Here the source j couples to a gauge dependent quantity, the field σ . Consequently, $\tilde{W}(T, j; J)$ is gauge dependent and not a physical observable. We have also kept the dependence on the source J . From $\tilde{W}(T, j; J)$ one obtains the effective potential $\tilde{V}(T, \varphi; J)$ via Legendre transformation, with $\varphi = \partial \tilde{W} / \partial j$. The wanted free energy density $W(T, J)$ can now be obtained from the effective potential \tilde{V} . In the infinite volume limit, one has

$$W(T, J) = \tilde{V}(T, \varphi_{min}(T, J), J) , \quad (10)$$

where $\varphi_{min}(T, J)$ is the global minimum of the effective potential $\tilde{V}(T, \varphi; J)$. For arbitrary values of φ the potential \tilde{V} is gauge dependent. However, its value at the minimum is known to be gauge independent, yielding a gauge independent free energy $W(T, J)$.

At the critical temperature T_c of a first-order transition the order parameter ρ ,

$$\frac{1}{2}\rho \equiv \frac{1}{\Omega} \int_{\Omega} d^3x \langle \hat{\Phi}^\dagger(x) \hat{\Phi}(x) \rangle = \frac{\partial}{\partial J} W(T, J) , \quad (11)$$

and the energy density E ,

$$E(T, J) = W(T, J) - T \frac{\partial}{\partial T} W(T, J) , \quad (12)$$

are discontinuous. The jump in the energy density is the latent heat ΔQ .

For the first-order phase transition from liquid to vapour there exists a well known relation between the latent heat and the change of the molar volume, the Clausius-Clapeyron equation [10]. In the electroweak phase transition the order parameter $\langle \Phi^\dagger \Phi \rangle$ plays the role of the molar volume, and a completely analogous relation can be derived.

The electroweak plasma can exist in two phases, the massive low-temperature Higgs phase with free energy $W_b(T, J)$ and the massless high-temperature symmetric phase with free energy $W_s(T, J)$. In the $J - T$ -plane the boundary between the two phases is determined by the equilibrium condition

$$W_s(T, J(T)) = W_b(T, J(T)) . \quad (13)$$

This equilibrium condition yields a useful connection between the latent heat ΔQ and the jump in the order parameter $\Delta \rho$. Using the definitions

$$\Delta Q = -T \frac{\partial}{\partial T} (W_s - W_b) \quad , \quad \Delta \rho = 2 \frac{\partial}{\partial J} (W_s - W_b) , \quad (14)$$

one easily obtains

$$\Delta Q = \frac{1}{2} \Delta \rho T \frac{dJ}{dT} . \quad (15)$$

This is the Clausius-Clapeyron equation of the electroweak phase transition. Together with a dimensional analysis it implies

$$\Delta Q = -\frac{1}{2} m_H^2 \Delta \rho (1 + \mathcal{O}(g^2, \lambda)) , \quad (16)$$

where $m_H = \sqrt{-2\mu^2}(1 + \mathcal{O}(g^2, \lambda))$ is the physical Higgs mass at zero temperature. This relation provides a useful check for perturbative as well as lattice results.

Perturbation theory

Near the ground state, $J = 0$, the free energy $W(T, J)$ can be evaluated as power series in the couplings g and λ by means of resummed perturbation theory which has been carried out up to two loops [11, 12, 8]. Here, thermal corrections are added to the tree-level masses of the scalar fields and the longitudinal component of the vector boson field,

$$\delta S_\beta = \beta \int d^3x \left(\frac{1}{2} \alpha_{01} T^2 (\sigma^2 + \pi^2) + \frac{1}{2} \alpha_1 T^2 W_L^2 \right) . \quad (17)$$

The sum of tree-level masses and thermal corrections then enters the boson propagators in loop diagrams, and $\delta S_\beta^c = -\delta S_\beta$ is treated as counter term. It turns out that the resummation of static modes only is a preferred procedure [11]. Hence, in Eq. (17) the fields σ and π do not depend on the imaginary time τ . To leading order in the couplings, one obtains for the parameters in Eq. (17) from one-loop self energy corrections $\alpha_{01} = \frac{3}{16}g^2 + \frac{1}{2}\lambda$, $\alpha_1 = \frac{5}{6}g^2$.

The masses of the boson propagators are obtained from Eqs. (4) and (17) by shifting the Higgs field σ by the average field φ . This yields m_L , m_T , m_σ and m_π for longitudinal and transverse part of the vector field, the Higgs field and the Goldstone field, respectively. The resummation procedure can be optimized by adding terms of higher order in the couplings to Eq. (17). In the Higgs phase, where one is only interested in the effective potential close to the minimum, the choice of a field dependent correction δS_β^b is useful which yields for the scalar masses,

$$m_\sigma^2 = 2\lambda\varphi^2 \quad , \quad m_\pi^2 = 0 \quad . \quad (18)$$

Hence, no thermal resummation for scalar masses is performed in the Higgs phase. In the symmetric phase it is useful to determine the scalar masses self-consistently by

$$m_\sigma^2 = m_\pi^2 = \frac{1}{\varphi} \frac{\partial}{\partial \varphi} \tilde{V}(T, 0; J) \quad . \quad (19)$$

For given vector boson masses m_L and m_T , this is a gap equation for the scalar masses, which can be solved at each order of the loop expansion.

Having specified the vector boson and scalar masses in the Higgs phase and in the symmetric phase, the free energy can be calculated from the effective potential \tilde{V} , using the relation (10). Its two local minima yield the free energy $W_s(T, J)$ and $W_b(T, J)$ in the symmetric phase and the Higgs phase, respectively. The free energy of the ground state is

$$W(T, 0) = \min\{W_s(T, 0), W_b(T, 0)\} \quad . \quad (20)$$

It is a concave function whose derivative is discontinuous at the critical temperature T_c . We can also consider the dependence of the free energy on the external source at the critical temperature T_c . This function, $W(T_c, J)$, is shown in Fig. 3. Here we have subtracted in both phases the huge linear term $T^2 J/6$, whose sole effect is to shift the expectation value $\langle \Phi^\dagger \Phi \rangle$ by $T^2/3$.

From the free energy $W(T, J)$ one can obtain the gauge invariant effective potential $V(T, \rho)$ by means of a Legendre transformation. Since the derivative of $W(T, J)$ is not continuous everywhere, one has to use the definition (see [13]),

$$V(T, \rho) = \sup_J \{W(T, J) - \frac{1}{2}\rho J\} \quad . \quad (21)$$

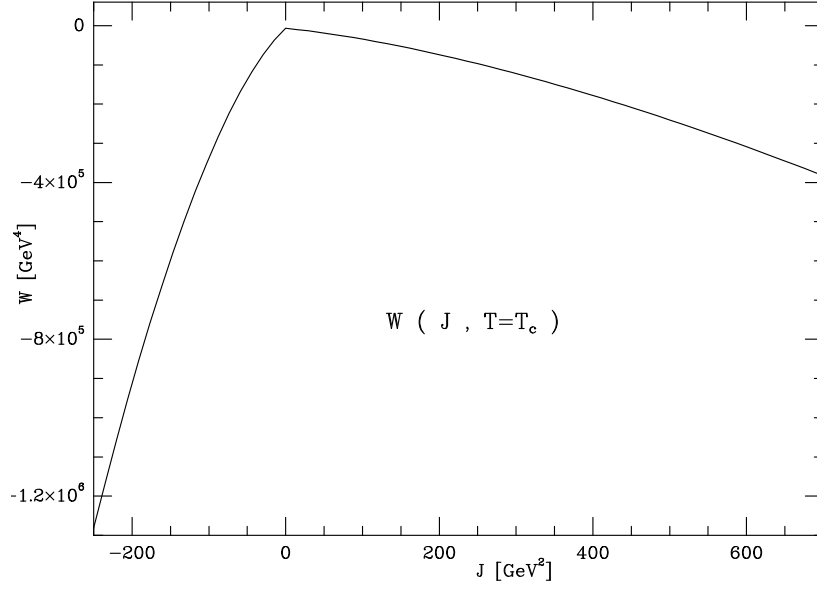


Figure 3: Free energy at the critical temperature as a function of the source J ($m_H = 70$ GeV).

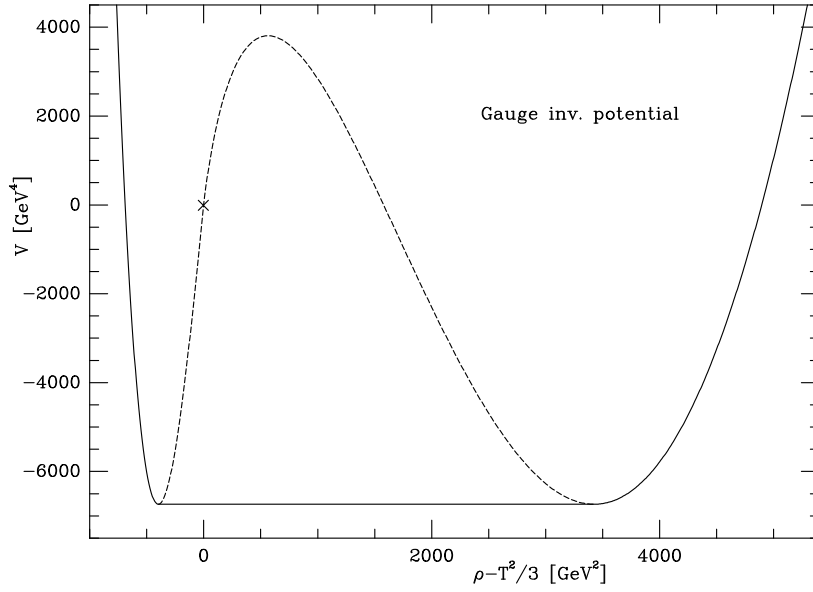


Figure 4: Gauge invariant effective potential (solid line) and its analytic continuations from the single phase regions into the mixed phase region (dashed line). The cross denotes the matching point.

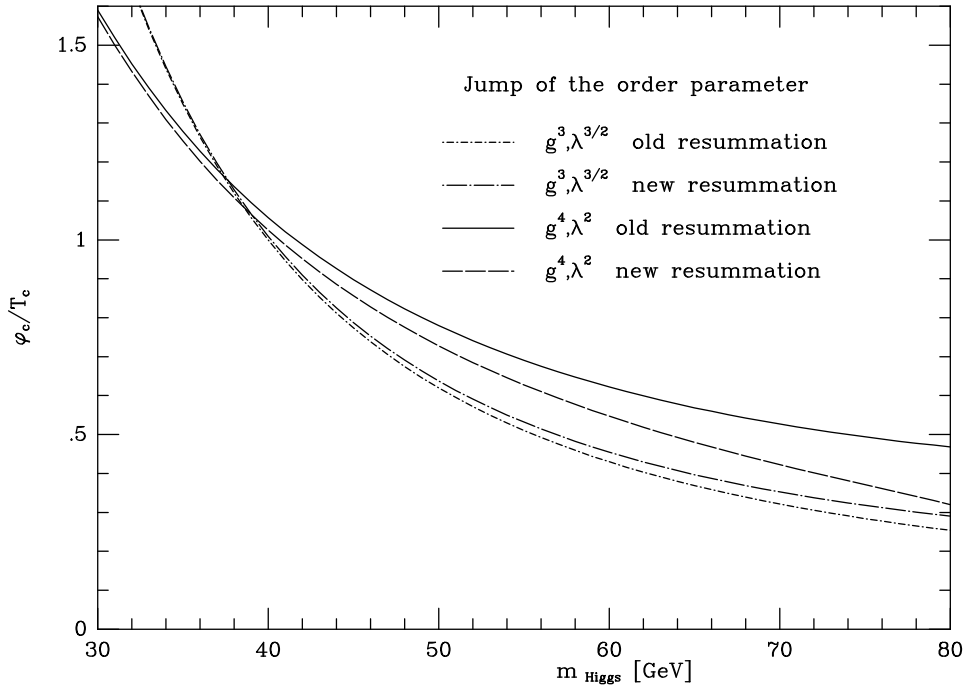


Figure 5: Jump of the order parameter $\varphi_c = \sqrt{\Delta\rho}$ in units of the critical temperature T_c .

This yields the convex, non-analytic function, which is plotted in Fig. 4 as full line. One may also compute the ordinary Legendre transform $V_s(T, \rho)$ and $V_b(T, \rho)$ of $W_s(T, J)$ and $W_b(T, J)$, respectively. V_s and V_b are also shown in Fig. 4. In the region outside of the two local minima, V_s and V_b , respectively, coincide with the convex effective potential $V(T, \rho)$. Between the two local minima, V_s and V_b represent two analytical continuations of $V(T, \rho)$, which meet at the ‘matching point’ $\rho_M = T^2/3$. At this point, marked by a cross in the plot, the first derivatives of both curves coincide.

The non-convex ‘effective potential’ obtained by combining V_s and V_b on both sides of the ‘matching point’ has a barrier between symmetric and Higgs phase like the ordinary effective potential $\tilde{V}(T, \varphi; J)$. Note, however, the difference in the range of fields. For \tilde{V} one has $0 \leq \varphi < \infty$, whereas for the potential V the field ρ varies in the range $-\infty < \rho < \infty$. The generation of a barrier between two local minima as analytic continuation from a convex effective potential is reminiscent of the treatment of first-order phase transitions in condensed matter physics [14]. However, the precise physical meaning of the resulting non-convex ‘effective potential’ still remains to be understood.

Comparison with lattice simulations

The asymmetric resummation described above has been carried out up to two-loop order. In the Higgs phase the scalar masses are given by Eq. (18), and in the symmetric phase they are self-consistently determined from Eq. (19). Note, that in the two-loop calculation the counter term to be inserted in the one-loop graph is $\mathcal{O}(g^3)$, whereas the scalar mass determined from Eq. (19) is of higher order in g .

In the symmetric phase the self-consistently determined scalar masses are infrared divergent. With $m_T = g\varphi/2$, the two-loop potential yields a contribution which diverges logarithmically at $\varphi \approx 0$,

$$m_\sigma^2 \simeq -\frac{33g^4}{128\pi^2} T^2 \ln \beta m_T. \quad (22)$$

Following [15] one may regularize this divergence by means of a ‘magnetic mass’ term. In Eq. (22) one substitutes $m_T^2 = g^2\varphi^2/4 + \gamma^2 g^4 T^2/(9\pi^2)$. In the following numerical results will be given for $\gamma = 1$, which is obtained by one-loop gap equations [15, 16]. The results change only insignificantly if the parameter γ is varied between 0.3 and 3.0. In addition to the resummation procedure one has to choose a renormalization scheme. A good choice is the $\overline{\text{MS}}$ -scheme with $\bar{\mu} = T$, supplemented by finite counter terms $\delta\mu^2$ and $\delta\lambda$ which account for the most important zero-temperature renormalization effects.

Given the two-loop potential in the symmetric phase and in the Higgs phase, one can numerically determine the critical temperature T_c , where the two potentials at their respective local minima are degenerate. Differentiation with respect to temperature and the external source J then yields latent heat and jump in the order parameter $\rho = 2\langle\Phi^\dagger\Phi\rangle$. The result for $\varphi_c = \sqrt{\Delta\rho}$ is shown in Fig. 5, labelled ‘new resummation’. Here the zero-temperature standard model values $m_W = 80$ GeV and $g^2 = 0.57$ have been used. In the case of the ‘old resummation’ [12] φ_c corresponds to the position of the second minimum. The one-loop potential is $\mathcal{O}(g^3, \lambda^{3/2})$, the two-loop potential is $\mathcal{O}(g^4, \lambda^2)$. As Fig. 5 illustrates, the ‘new resummation’ procedure improves the convergence significantly. The relative change of an observable from one-loop to two-loop may be characterized by $\delta = 2|O_1 - O_2|/(O_1 + O_2)$. For the jump in the order parameter φ_c , δ increases from ~ 0.01 at $m_H = 40$ GeV to ~ 0.2 at $m_H = 70$ GeV. Above $m_H \sim 80$ GeV the convergence deteriorates rapidly, and the perturbative calculation is no longer self-consistent.

Observables of the four-dimensional SU(2) Higgs model at finite temperature can be directly computed by means of Monte Carlo simulations on lattices with spatial size L_s and temporal size $L_t \ll L_s$. Such finite temperature simulations at small values of λ were initiated in [17], and high statistics simulations were performed in [18, 19]. For the two Higgs masses $m_H \simeq 18$ GeV and $m_H \simeq 49$ GeV the quantities T_c , ΔQ and $\varphi_c \equiv v_T$ were computed on $L_t = 2$ and $L_t = 3$ lattices, and for $m_H \simeq 35$ GeV a detailed study of the first-order phase transition was carried out on lattices of temporal size up to $L_t = 5$.

In a complementary approach detailed studies have also been carried out based on dimensional reduction where non-zero Matsubara frequencies are first integrated out perturbatively. Recent results on dimensional reduction are described in [20, 21] where also references to previous work can be found. Numerical simulations were performed for the effective three dimensional theory which led to a quantitative description of the first-order phase transition for Higgs masses up to ~ 70 GeV [22, 23].

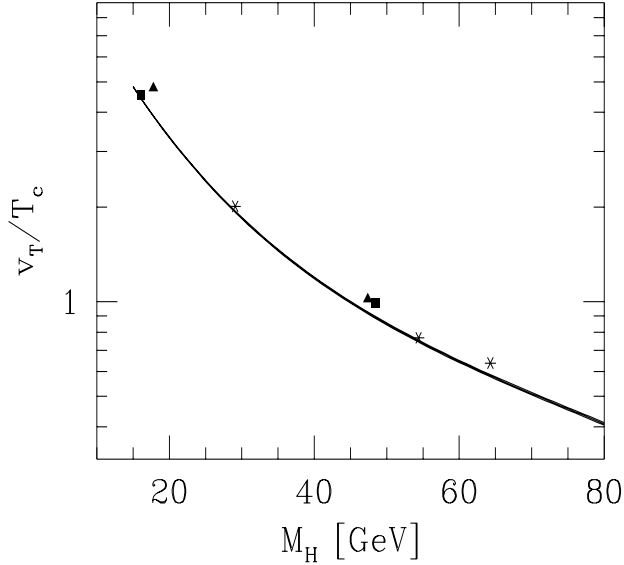


Figure 6: Jump of the order parameter at the critical temperature. Comparison of four-dimensional simulations (triangles, squares [18]) with three-dimensional simulations (stars [22]) and perturbation theory [8]. From [24].

In Fig. 6 results for the jump in the order parameter, $\Delta v(T_c) \equiv v_T$, are compared [24], which were obtained by simulations of the four-dimensional theory [18], the three-dimensional theory [22] and perturbation theory [8], respectively. The comparison is made for the parameter values $M_W = 80$ GeV and $g = 0.57$. The statistical errors of the numerical simulations are so small that they are invisible in the figure. The agreement between the three approaches is remarkable and certainly better than the systematic uncertainties of perturbation theory (cf. Fig. 5). The continuum limit for the critical temperature has been studied in detail in [19] for $m_H \simeq 34$ GeV, i.e., $R_{HW} = M_H/M_W \simeq 0.42$. The results are shown in Fig. 7, where the error bars include the statistical error and an estimate of the systematic error. A comparison is made with perturbation theory and the three-dimensional simulation. The lattice simulations yield a critical temperature slightly below the result from perturbation theory, but the difference is not significant.

The agreement between results from perturbation theory and non-perturbative

lattice simulations is surprising, since in the symmetric phase perturbation theory is known to be infrared divergent, which prevents a straightforward extension of the present two-loop calculation to three loops. The infrared behaviour of a running gauge coupling has been studied in [26]. In the symmetric phase the scalar masses depend logarithmically on an infrared cutoff of order the magnetic scale $\sim g^2 T$. This is reminiscent of the Debye screening length in pure gauge theory which, at two-loop order, also requires an infrared cutoff $\sim g^2 T$ [27]. Here, a non-perturbative definition of the Debye screening length can be given such that the dominant contribution is given by the perturbative result and an additional non-perturbative contribution can be evaluated in a well-defined manner [28]. Such a split into a dominant perturbative contribution and a non-perturbative remainder should also be possible for the free energy in the symmetric phase. This would then justify the perturbative treatment of the first-order electroweak phase transition. For the pure gauge theory this problem has been discussed in [29].

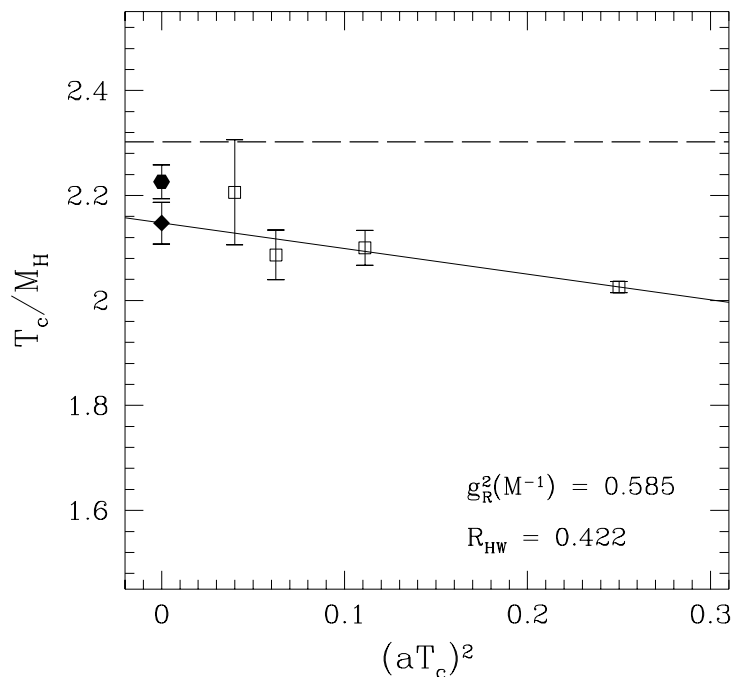


Figure 7: Numerical results for the ratio of critical temperature and Higgs boson mass versus $(aT_c)^2 = L_t^{-2}$; the full line is the extrapolation to the continuum limit [19]. The dashed horizontal line shows the prediction of two-loop perturbation theory [8]. The hexagon between continuum limit and perturbation theory represents the result of a three-dimensional simulation [22], adjusted to the parameters of the four-dimensional calculation [25].

Perturbation theory in the symmetric phase fails with respect to correlation lengths of gauge-invariant vector and scalar fields. Lattice simulations yield shorter correlation lengths for vector fields in the symmetric phase than in the Higgs phase [18, 22, 24, 30, 23]. The contrary is true for the correlation length of the vector field evaluated in a fixed gauge [31, 32] - a puzzle which still remains to be resolved. The latter screening lengths appear to be related to the critical Higgs mass $m_H \sim 80$ GeV where the first-order phase transition turns into a smooth crossover [31, 33, 34].

Independent of the intriguing non-perturbative features of the symmetric phase, which require further studies, it is now known that the necessary condition (3) for electroweak baryogenesis is not satisfied in the standard model. For Higgs boson masses above the present experimental bound of 58 GeV [35] one has according to Fig. 6,

$$\frac{\Delta v(T_c)}{T_c} < 0.7, \quad (23)$$

which is much smaller than the lower bound (3). For appropriate choices of parameters it is possible to satisfy this bound in some extensions of the standard model, but in these models it has not been demonstrated that electroweak baryogenesis is indeed possible. This strongly suggests that the baryon asymmetry has been generated in the high-temperature phase of the standard model, as it is the case for instance in conventional grand unified theories.

3 Baryogenesis via leptogenesis

In the high temperature phase of the standard model the asymmetries of baryon number and lepton number are proportional in thermal equilibrium (cf. (2)),

$$\langle B \rangle_T \simeq C \langle B - L \rangle_T \simeq \frac{C}{C - 1} \langle L \rangle_T.$$

In the standard model, as well as its unified extension based on the group SU(5), $B - L$ is conserved. Hence, no asymmetry in $B - L$ can be generated, and $\langle B \rangle_T$ vanishes. Furthermore, as discussed above, baryogenesis at the electroweak phase transition appears unlikely. As a consequence, the non-vanishing of the baryon asymmetry is a strong argument for lepton number violation. This is naturally realized by adding right-handed Majorana neutrinos to the standard model. This extension of the standard model can be embedded into grand unified theories with gauge groups containing SO(10) [36]. Heavy right-handed Majorana neutrinos can also explain the smallness of the light neutrino masses via the see-saw mechanism [37].

The connection between baryon number and lepton number at high temperatures can be used to generate a baryon asymmetry. This was suggested by Fukugita and Yanagida [38]. The primordial lepton asymmetry is generated by the out-of-equilibrium decay of heavy Majorana neutrinos in the standard manner. This mechanism has subsequently been studied by several authors [39, 40, 41], and it has been

shown that the observed baryon asymmetry (cf. [42]),

$$Y_B = \frac{n_B}{s} = (0.6 - 1) \cdot 10^{-10}, \quad (24)$$

can be obtained for a wide range of parameters.

In unified theories with right-handed neutrinos $B - L$ is in general spontaneously broken. Unification also restricts the new parameters which are introduced by adding right-handed neutrinos to the standard model. In $SO(10)$ unification it is natural to assume a similar pattern of mixings and masses for leptons and quarks. This ansatz, together with the requirement of baryogenesis, also restricts the scale of $B - L$ breaking. The following discussion is closely related to [43].

The most general lagrangian for couplings and masses of charged leptons and neutrinos is given by

$$\mathcal{L}_Y = -\bar{l}_L \tilde{\phi} g_l e_R - \bar{l}_L \phi g_\nu \nu_R - \frac{1}{2} \bar{\nu}_R^C M \nu_R + \text{h.c.}, \quad (25)$$

where $l_L = (\nu_L, e_L)$ is the left-handed lepton doublet and $\phi = (\phi^0, \phi^-)$ is the standard model Higgs doublet. The vacuum expectation value of the Higgs field $\langle \phi \rangle = v \neq 0$ generates Dirac masses m_l and m_D for charged leptons and neutrinos,

$$m_l = g_l v \quad \text{and} \quad m_D = g_\nu v, \quad (26)$$

which are assumed to be much smaller than the Majorana masses M . This yields light and heavy neutrinos

$$\nu \simeq K^\dagger \nu_L + \nu_L^C K \quad , \quad N \simeq \nu_R + \nu_R^C, \quad (27)$$

with masses

$$m_\nu \simeq -K^\dagger m_D \frac{1}{M} m_D^T K^* \quad , \quad m_N \simeq M, \quad (28)$$

as mass eigenstates. Here K is a unitary matrix which relates weak and mass eigenstates. Since the heavy neutrinos N_i are Majorana fermions, their decay to lepton and Higgs scalar violates lepton number. In the rest system the decay width of N_i reads at tree level,

$$\Gamma_{Di} := \Gamma_{rs} (N^i \rightarrow \phi^\dagger + l) + \Gamma_{rs} (N^i \rightarrow \phi + \bar{l}) = \frac{M_i (m_D^\dagger m_D)_{ii}}{8\pi v^2}. \quad (29)$$

Interference between tree level and one-loop amplitudes (cf. Fig. 8) yields the CP asymmetry [41]

$$\epsilon_i = \frac{1}{8\pi v^2 (m_D^\dagger m_D)_{ii}} \sum_j \text{Im} \left[(m_D^\dagger m_D)_{ij}^2 \right] f \left(\frac{M_j^2}{M_i^2} \right) \quad (30)$$

with $f(x) = \sqrt{x} \left[1 - (1+x) \ln \left(\frac{1+x}{x} \right) \right]$.

The corresponding maximal $B - L$ asymmetry is $\epsilon_i/g*$, where $g*$ is the number of relativistic degrees of freedom (cf. [42]).

In order to generate the observed baryon asymmetry several conditions have to be fulfilled. First, the CP asymmetry ϵ_i has to be large enough; second, the out-of-equilibrium condition $\Gamma_{Di} < \kappa H(T = M_i)$ for the decaying heavy neutrino has to be fulfilled, where H is the Hubble parameter; third, the L violating interactions have to be sufficiently weak in order not to erase the generated lepton asymmetry. These conditions tend to favour small masses for the light neutrinos and a large scale of $B - L$ breaking [44]. However, these constraints are not model independent. The corresponding bounds on the light neutrino masses can be considerably relaxed if appropriate chiral symmetries are effectively conserved in some temperature range in the symmetric phase [45].

All these conditions are automatically taken into account if one integrates the Boltzmann equations including all relevant interactions for the model under consideration. The results discussed below are based on such an analysis using the Boltzmann equations described in [41]. All three heavy neutrino families are taken into account as intermediate states whereas only the asymmetry generated by the lightest of the right-handed neutrinos is relevant, since the asymmetries generated by the heavier neutrinos are washed out.

Neutrino masses and mixings

Let us now consider a similar pattern of mixings and mass ratios for leptons and quarks, which is natural in $SO(10)$ unification. Such an ansatz is most transparent in a basis where all mass matrices are maximally diagonal. In addition to real mass eigenvalues two mixing matrices appear. One can always choose a basis for the lepton fields such that the mass matrices m_l for the charged leptons and M for the heavy

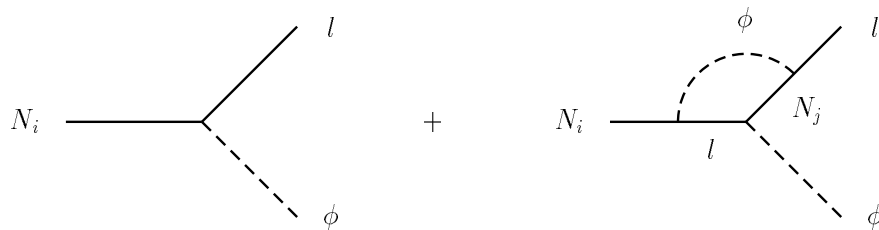


Figure 8: Contributions to the decay of a heavy Majorana neutrino

Majorana neutrinos N_i are diagonal with real and positive eigenvalues,

$$m_l = \begin{pmatrix} m_e & 0 & 0 \\ 0 & m_\mu & 0 \\ 0 & 0 & m_\tau \end{pmatrix} \quad M = \begin{pmatrix} M_1 & 0 & 0 \\ 0 & M_2 & 0 \\ 0 & 0 & M_3 \end{pmatrix}. \quad (31)$$

In this basis m_D is a general complex matrix, which can be diagonalized by a biunitary transformation. Therefore, we can write m_D in the form

$$m_D = V \begin{pmatrix} m_1 & 0 & 0 \\ 0 & m_2 & 0 \\ 0 & 0 & m_3 \end{pmatrix} U^\dagger, \quad (32)$$

where V and U are unitary matrices and the m_i are real and positive. In the absence of a Majorana mass term V and U would correspond to Kobayashi-Maskawa type mixing matrices of left- and right-handed charged currents, respectively.

According to Eqs. (29) and (30) the CP asymmetry is determined by the mixings and phases present in the product $m_D^\dagger m_D$, where the matrix V drops out. Therefore, to leading order, the mixings and phases which are responsible for baryogenesis are entirely determined by the matrix U . Correspondingly, the mixing matrix K in the leptonic charged current, which determines CP violation and mixings of the light leptons, depends on mass ratios and mixing angles and phases of U and V . Hence, there is no direct connection between the CP violation and generation mixing at high and low energies.

Consider now the mixing matrix U . One can factor out five phases, which yields

$$U = e^{i\gamma} e^{i\lambda_3\alpha} e^{i\lambda_8\beta} U_1 e^{i\lambda_3\sigma} e^{i\lambda_8\tau}, \quad (33)$$

where the λ_i are the Gell-Mann matrices. The remaining matrix U_1 depends on three mixing angles and one phase, like the Kobayashi-Maskawa matrix for quarks. In analogy to the quark mixing matrix we choose the Wolfenstein parametrization [46] as ansatz for U_1 ,

$$U_1 = \begin{pmatrix} 1 - \frac{\lambda^2}{2} & \lambda & A\lambda^3(\rho - i\eta) \\ -\lambda & 1 - \frac{\lambda^2}{2} & A\lambda^2 \\ A\lambda^3(1 - \rho - i\eta) & -A\lambda^2 & 1 \end{pmatrix}, \quad (34)$$

where A and $|\rho + i\eta|$ are of order one, while the mixing parameter λ is assumed to be small. For the masses m_i and M_i we assume a hierarchy like for up-type quarks,

$$m_1 = b\lambda^4 m_3 \quad m_2 = c\lambda^2 m_3 \quad b, c = \mathcal{O}(1) \quad (35)$$

$$M_1 = B\lambda^4 M_3 \quad M_2 = C\lambda^2 M_3 \quad B, C = \mathcal{O}(1). \quad (36)$$

For the eigenvalues m_i of the Dirac mass matrix this choice is motivated by $SO(10)$ unification. The masses M_i cannot be degenerate, because in this case there exists a

basis for ν_R such that $U = 1$, which implies that no baryon asymmetry is generated. For simplicity the masses M_i are assumed to scale like the Dirac neutrino masses.

The light neutrino masses are given by the seesaw formula (28). The matrix K , which diagonalises the neutrino mass matrix, can be evaluated in powers of λ . A straightforward calculation gives the following masses for the light neutrino mass eigenstates

$$m_{\nu_e} = \frac{b^2}{|C + e^{4i\alpha} B|} \lambda^4 m_{\nu_\tau} + \mathcal{O}(\lambda^6) \quad (37)$$

$$m_{\nu_\mu} = \frac{c^2 |C + e^{4i\alpha} B|}{BC} \lambda^2 m_{\nu_\tau} + \mathcal{O}(\lambda^4) \quad (38)$$

$$m_{\nu_\tau} = \frac{m_3^2}{M_3} + \mathcal{O}(\lambda^4) . \quad (39)$$

The CP -asymmetry in the decay of the lightest right-handed neutrino N_1 is easily obtained from Eqs. (30) and (34)-(36),

$$\epsilon_1 = - \frac{1}{16\pi} \frac{B A^2}{c^2 + A^2 |\rho + i\eta|^2} \lambda^4 \frac{m_3^2}{v^2} \text{Im} [(\rho - i\eta)^2 e^{i2(\alpha + \sqrt{3}\beta)}] + \mathcal{O}(\lambda^6) . \quad (40)$$

This yields for the magnitude of the CP asymmetry,

$$|\epsilon_1| \leq \frac{1}{16\pi} \frac{B A^2 |\rho + i\eta|^2}{c^2 + A^2 |\rho + i\eta|^2} \lambda^4 \frac{m_3^2}{v^2} + \mathcal{O}(\lambda^6) . \quad (41)$$

How close the value of $|\epsilon_1|$ is to this upper bound depends on the phases α , β and $\arg(\rho + i\eta)$. Since $\epsilon_1 \propto m_3^2/v^2$, one can already conclude that a large value of the Yukawa coupling m_3/v will be preferred by this mechanism of baryogenesis. This holds irrespective of the neutrino mixings.

Numerical results

To obtain a numerical value for the produced baryon asymmetry, one has to specify the free parameters in the ansatz (34)-(36). In the following we will use as a constraint the value for the ν_μ -mass which is preferred by the MSW explanation [47] of the solar neutrino deficit (cf. [48]),

$$m_{\nu_\mu} \simeq 3 \cdot 10^{-3} \text{ eV} . \quad (42)$$

A generic choice for the free parameters is to take all $\mathcal{O}(1)$ parameters equal to one and to fix λ to a value which is of the same order as the λ parameter of the quark mixing matrix,

$$A = B = C = b = c = |\rho + i\eta| \simeq 1 , \quad \lambda \simeq 0.1 . \quad (43)$$

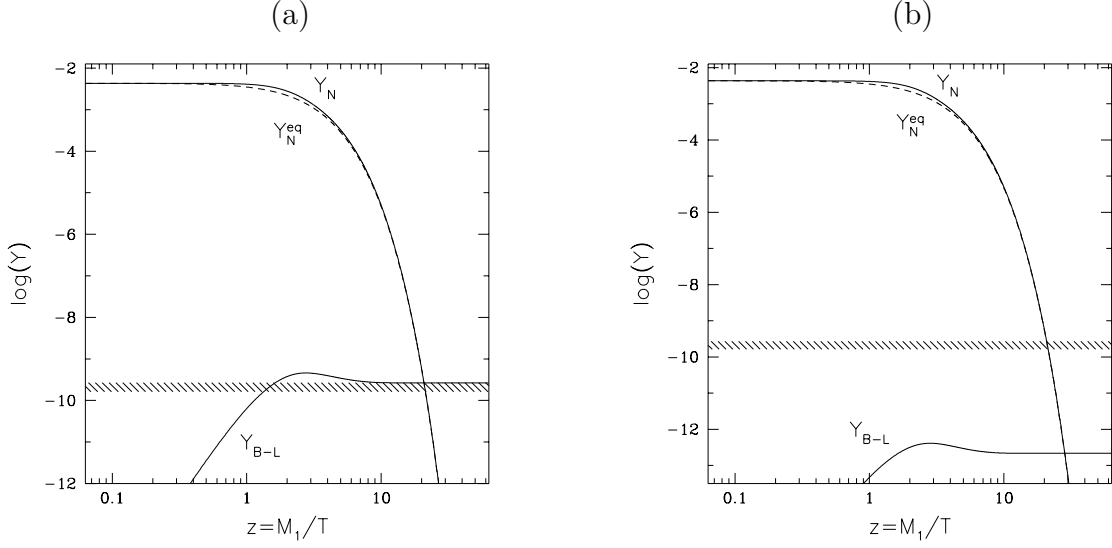


Figure 9: *Time evolution of the neutrino number density and the $B - L$ asymmetry for $\lambda = 0.1$ and for $m_3 = m_t$ (a) or $m_3 = m_b$ (b). The equilibrium distribution for N_1 is represented by a dashed line, while the hatched area shows the measured value for the asymmetry.*

From Eqs. (37)-(39), (42) and (43) one now obtains,

$$m_{\nu_e} \simeq 8 \cdot 10^{-6} \text{ eV} , \quad m_{\nu_\tau} \simeq 0.15 \text{ eV} . \quad (44)$$

Finally, a second mass scale has to be specified. In unified theories based on $\text{SO}(10)$ the Dirac neutrino mass m_3 is naturally equal to the top-quark mass,

$$m_3 = m_t \simeq 174 \text{ GeV} . \quad (45)$$

This determines the masses of the heavy Majorana neutrinos N_i ,

$$M_3 \simeq 2 \cdot 10^{14} \text{ GeV} , \quad (46)$$

and, consequently, $M_1 \simeq 2 \cdot 10^{10} \text{ GeV}$ and $M_2 \simeq 2 \cdot 10^{12} \text{ GeV}$. From Eq. (41) one obtains the CP asymmetry $|\epsilon_1| \simeq 10^{-6}$, where we have assumed maximal phases. The solution of the set of Boltzmann equations described in [41] now yields the $B - L$ asymmetry (see Fig. 9a),

$$Y_{B-L} \simeq 3 \cdot 10^{-10} , \quad (47)$$

which is indeed the correct order of magnitude. The precise value depends on unknown phases.

The large mass M_3 of the heavy Majorana neutrino N_3 (cf. (46)), suggests that $B - L$ is already broken at the unification scale $\Lambda_{\text{GUT}} \sim 10^{16} \text{ GeV}$, without any intermediate scale of symmetry breaking. This large value of M_3 is a consequence of

the choice $m_3 \simeq m_t$. To test the sensitivity of the result for Y_{B-L} on this assumption, consider the alternative choice, $m_3 = m_b \simeq 4.5$ GeV, with all other parameters remaining unchanged. In this case one obtains $M_3 = 10^{11}$ GeV and $|\epsilon_1| = 5 \cdot 10^{-10}$ for the mass of N_3 and the CP asymmetry, respectively. Since the maximal $B - L$ asymmetry is $-\epsilon_1/g_*$ (cf. [42]), it is clear that the generated asymmetry will be too small. The solutions of the Boltzmann equations are shown in Fig. 9b. The generated asymmetry, $Y_{B-L} \simeq 2 \cdot 10^{-13}$, is too small by more than two orders of magnitude. We conclude that high values for both masses m_3 and M_3 are preferred, which is natural in $SO(10)$ unification.

Models for dark matter involving massive neutrinos favour a τ -neutrino mass $m_{\nu_\tau} \simeq 5$ eV [49], which is significantly larger than the value given in (44). Such a large value for the τ -neutrino mass can be accommodated within the ansatz described in this section. However, it does not correspond to the simplest choice of parameters and requires some fine-tuning. For the mass of the heaviest Majorana neutrino one obtains in this case $M_3 \simeq 6 \cdot 10^{12}$ GeV.

Without an intermediate scale of symmetry breaking, the unification of gauge couplings appears to require low-energy supersymmetry. This provides further sources for generating a $B - L$ asymmetry [50], whose size depends on additional assumptions. In this case, especially constraints on the reheating temperature [42] and the possible role of preheating [51] require further studies.

4 Conclusions

The observation that baryon and lepton number violating processes are in thermal equilibrium in the high-temperature phase of the standard model, is of crucial importance for the theory of baryogenesis. In particular it implies that the presently observed cosmological baryon asymmetry has been finally determined at the electroweak phase transition.

During the past three years a quantitative understanding of the first-order electroweak phase transition for Higgs boson masses up to $m_H \sim 70$ GeV has been achieved by means of analytical and numerical methods. The transition to a crossover near $m_W \sim m_H$ and the full understanding of the high-temperature phase still require further work. However, already now we know that for Higgs boson masses above the lower bound obtained at LEP, baryogenesis at the weak electroweak transition is very unlikely.

Searching for alternatives to electroweak baryogenesis the connection between baryon number and lepton number in the symmetric phase is again crucial. It allows to generate the baryon asymmetry from a lepton asymmetry, as suggested by Fukugita and Yanagida. Necessary ingredients are right-handed neutrinos and Majorana masses, which appear naturally in $SO(10)$ unified theories. The example described in the previous section demonstrates that this mechanism can explain the observed cosmological baryon asymmetry without any fine-tuning of parameters.

Further sources for generating a lepton asymmetry exist in models with low-energy supersymmetry. All this suggests that, hoping for further progress in theory and new experimental results on neutrino properties, we can look forward to an intriguing interplay between non-perturbative processes in the standard model, early universe cosmology and neutrino physics.

Acknowledgements

It is a pleasure to thank Z. Fodor, A. Hebecker and M. Plümacher for an enjoyable collaboration which led to the results described in this report. I would also like to thank J. Hein, K. Jansen and I. Montvay for their continuous help in understanding lattice results and for many valuable discussions. Last, but not least, I would like to thank the organizers of *Quarks '96* for a stimulating meeting and also for hospitality in Yaroslavl.

References

- [1] D. A. Kirzhnits, JETP Lett. 15 (1972) 529;
D. A. Kirzhnits and A. D. Linde, Phys. Lett. B42 (1972) 471
- [2] G. 't Hooft, Phys. Rev. Lett. 37 (1976) 8
- [3] V. A. Kuzmin, V. A. Rubakov and M. E. Shaposhnikov, Phys. Lett. B155 (1985) 36
- [4] S. Yu. Khlebnikov and M. E. Shaposhnikov Nucl. Phys. B308 (1988) 885
- [5] B. I. Halperin, T. C. Lubensky and S.-K. Ma, Phys. Rev. Lett. 32 (1974) 292
- [6] D. A. Kirzhnits and A. D. Linde, Ann. of Phys. 101 (1976) 195
- [7] For a discussion and references, see
A. G. Cohen, D. B. Kaplan and A. E. Nelson, Annu. Rev. Nucl. Part. Sci. 43 (1993) 27;
V. A. Rubakov and M. E. Shaposhnikov, Usp. Fis. Nauk. 166 (1996) 493
- [8] W. Buchmüller, Z. Fodor and A. Hebecker, Nucl. Phys. B447 (1995) 131
- [9] J.I. Kapusta, *Finite-temperature field theory* (Cambridge Univ. Press, 1989)
- [10] H. B. Callan, *Thermodynamics* (Wiley, New York, 1960)
- [11] P. Arnold and O. Espinosa, Phys. Rev. D47 (1993) 3546; D50 (1994) 6662 (E)
- [12] Z. Fodor and A. Hebecker, Nucl. Phys. B432 (1994) 127
- [13] L. O’Raifeartaigh, A. Wipf and H. Yoneyama, Nucl. Phys. B271 (1986) 653
- [14] J.S. Langer, Physica A73 (1974) 61
- [15] W. Buchmüller, Z. Fodor, T. Helbig and D. Walliser, Ann. Phys. 234 (1994) 260
- [16] J. R. Espinosa, M. Quirós and F. Zwirner, Phys. Lett. B314 (1993) 206
- [17] B. Bunk, E.-M. Ilgenfritz, J. Kripfganz and A. Schiller, Nucl. Phys. B403 (1993) 453
- [18] Z. Fodor, J. Hein, K. Jansen, A. Jaster and I. Montvay, Nucl. Phys. B439 (1995) 147
- [19] F. Csikor, Z. Fodor, J. Hein, A. Jaster and I. Montvay, Nucl. Phys. B474 (1996) 421
- [20] A. Kerres, G. Mack and G. Palma, Nucl. Phys. B467 (1996) 510

- [21] A. Jakovác and A. Patkós, hep-ph/9609364
- [22] K. Kajantie, M. Laine, K. Rummukainen and M. Shaposhnikov, Nucl. Phys. B466 (1996) 189
- [23] M. Gürtler, H. Perlt, A. Schiller, E.-M. Ilgenfritz and J. Kripfganz, DESY 96-113, hep-lat/9605042
- [24] K. Jansen, Nucl. Phys. B (Proc. Suppl.) 47 (1996) 196
- [25] M. Laine, HD-THEP-96-08, hep-lat/9604011
- [26] M. Reuter and C. Wetterich, Nucl. Phys. B408 (1993) 91
- [27] A. K. Rebhan, Nucl. Phys. B430 (1994) 319
- [28] P. Arnold and L. G. Yaffe, Phys. Rev. D52 (1995) 7208
- [29] E. Braaten and A. Nieto, Phys. Rev. D53 (1995) 3421
- [30] O. Philipsen, M. Teper and H. Wittig, Nucl. Phys. B469 (1996) 445
- [31] W. Buchmüller and O. Philipsen, Nucl. Phys. B443 (1995) 47
- [32] F. Karsch, T. Neuhaus, A. Patkós and J. Rank, Nucl. Phys. B474 (1996) 217
- [33] K. Kajantie, M. Laine, K. Rummukainen and M. Shaposhnikov, Phys. Rev. Lett. 77 (1996) 2887
- [34] K. Rummukainen, hep-lat/9608079
- [35] *Review of Particle Properties*, Phys. Rev. D54 (1996) 1
- [36] H. Fritzsch and P. Minkowski, Ann. Phys. 93 (1975) 193; H. Georgi, *Particles and Fields*, (AIP, NY, 1975), ed. C. E. Carlson, p. 575
- [37] T. Yanagida, in *Workshop on Unified Theories* (KEK report 79-18, 1979), eds. O. Sawada and A. Sugamoto, p. 95
M. Gell-Mann et al., in *Supergravity* (North Holland, Amsterdam, 1979), eds. P. van Nieuwenhuizen and D. Freedman, p. 315
- [38] M. Fukugita and T. Yanagida, Phys. Lett. B174 (1986) 45
- [39] M. A. Luty, Phys. Rev. D45 (1992) 455
- [40] P. Langacker, R. D. Peccei and T. Yanagida, Mod. Phys. Lett. A1 (1986) 541; T. Gherghetta and G. Jungman, Phys. Rev. D48 (1993) 1546; M. Flanz, E. A. Paschos and U. Sarkar, Phys. Lett. B345 (1995) 248; M. P. Worah, Phys. Rev. D53 (1996) 3902

- [41] M. Plümacher, DESY preprint 96-052, hep-ph/9604229, to appear in Z. Phys. C
- [42] For a review and references, see E. W. Kolb and M. S. Turner, *The Early Universe*, (Addison-Wesley, Redwood City, CA, 1990)
- [43] W. Buchmüller and M. Plümacher, DESY 96-158, hep-ph/9608308, to appear in Phys. Lett. B
- [44] M. Fukugita and T. Yanagida, Phys. Rev. D42 (1990) 3344; A. E. Nelson and S. M. Barr, Phys. Lett. B246 (1990) 141; J. Harvey and M. S. Turner, Phys. Rev. D42 (1990) 3344; B. A. Campbell, S. Davidson, J. Ellis and K. A. Olive, Phys. Lett. B256 (1991) 457; W. Fischler, G. F. Giudice, R. G. Leigh and S. Paban Phys. Lett. B258 (1991) 45; W. Buchmüller and T. Yanagida, Phys. Lett. B302 (1993) 240
- [45] L. E. Ibáñez and F. Quevedo, Phys. Lett. B283 (1992) 261; J. M. Cline, K. Kainulainen, and K. A. Olive, Phys. Rev. Lett. 71 (1993) 2372
- [46] L. Wolfenstein, Phys. Rev. Lett. 51 (1983) 1945
- [47] L. Wolfenstein, Phys. Rev. D17 (1978) 2369; S. P. Mikheyev and A. Y. Smirnov, Nuovo Cim. 9C (1986) 17
- [48] T. A. Kirsten, Ann. New York Acad. of Sci. 759 (1995) 1
- [49] G. Raffelt, preprint MPI-PTh/95-115, astro-ph/9511041
- [50] H. Murayama et al., Phys. Rev. Lett. 70 (1993) 1912; B. A. Campbell, S. Davidson and K. A. Olive, Nucl. Phys. B399 (1993) 111; L. Covi, E. Roulet and F. Vissani, preprint IC/96/73, hep-ph/9605319; H. Murayama and T. Yanagida, Phys. Lett. B322 (1994) 349; M. Dine, L. Randall and S. Thomas, Nucl. Phys. B458 (1996) 291
- [51] E. W. Kolb, A. Linde and A. Riotto, FERMILAB-PUB-96/133-A (1996); G. W. Anderson, A. Linde and A. Riotto, FERMILAB-PUB-96/078-A (1996)